Struct Chem (2010) 21:681–690
DOI 10.1007/s11224-010-9598-6

ORIGINAL RESEARCH

The proton transfer process observed in the structure analysis and DFT calculations of (*E*)-2-ethoxy-6-[(2-methoxyphenylimino)methyl]phenol

Hande Petek · Çiğdem Albayrak · Mustafa Odabaşoğlu · İsmet Şenel · Orhan Büyükgüngör

Received: 18 September 2009 / Accepted: 8 February 2010 / Published online: 10 March 2010

Abstract The crystal and molecular structures of an *o*-hydroxy Schiff base derivative, (*E*)-2-ethoxy-6-[(2-methoxyphenylimino)methyl]phenol, have been determined by single crystal X-ray diffraction analyses at 296 and 100 K. The results from temperature-dependent structural analysis regarding the tautomeric equilibrium of the compound were interpreted with the aid of quantum chemical calculations. To clarify the tautomerization process and its effects on the molecular geometry, the gas-phase geometry optimizations of two possible tautomers of the title molecule, its OH and NH form, were achieved using DFT calculations with B3LYP method by means of 6-31 + G(d,p) basis set. In order to describe the potential barrier belonging to the phenolic proton transfer, nonadiabatic Potential Energy Surface (PES) scan was performed based on the optimized geometry of the OH tautomeric form by varying the redundant internal coordinate, O–H bond distance. The Harmonic Oscillator Model of Aromaticity (HOMA) indices were calculated in every step of the scan process so as to express the deformation in the aromaticities of principal molecular moieties of the compound. The results show that there is a dynamic equilibrium between the aromaticity level of phenol and chelate ring and furthermore π-electron coupling affecting overall molecule of the title compound. Charge transfer from phenol ring to pseudo-aromatic chelate ring increases with increasing temperature, whereas π-electron transfer from chelate ring to anisole ring is decreased as temperature increases. The most strength intramolecular H-bonds are observed for conformers close to transition state.

Keywords Schiff base · Tautomerism · SUMP instruction · HOMA · PES scan · Crystal structure

Introduction

Schiff bases have been widely used as organic ligands in coordination chemistry due to their versatile abilities such as metal binding and chelating. In Schiff base complexes of both transition and *p*-block metals, which catalyze a wide variety of reactions [1, 2], the coordination environment can be modified by attaching different substituents to the ligand in order to provide a useful range of steric and electrostatic properties essential for the fine-tuning of their structure and reactivity. In addition, Schiff bases are one of the important classes of organic compounds and have extensive applications in biological function materials [3, 4], polymer ultraviolet stabilizers [5, 6] and laser dyes [7], as well as molecular switches in logic or memory circuits [8].

o-Hydroxy Schiff bases display two well-known tautomeric forms, phenol-imine (benzenoid), and keto-amine (quinoid). Except for these, another structural form known as the zwitterion is also observed [9, 10]. Zwitterionic forms of *o*-hydroxy Schiff bases are regarded as a variant

Electronic supplementary material The online version of this article (doi:10.1007/s11224-010-9598-6) contains supplementary material, which is available to authorized users.

H. Petek (✉) · İ. Şenel · O. Büyükgüngör
Department of Physics, Ondokuz Mayıs University, 55139-Kurupelit Samsun, Turkey
e-mail: hpetek@omu.edu.tr

Ç. Albayrak
Faculty of Education, Sinop University, 57000 Sinop, Turkey

M. Odabaşoğlu
Denizli Higher Vocational School, Chemistry Program, Pamukkale University, 20159 Denizli, Turkey

Scheme 1 Proton transfer equilibrium in *o*-hydroxy Schiff bases. *Dashed bonds* in NH tautomer indicate intermediate bonds

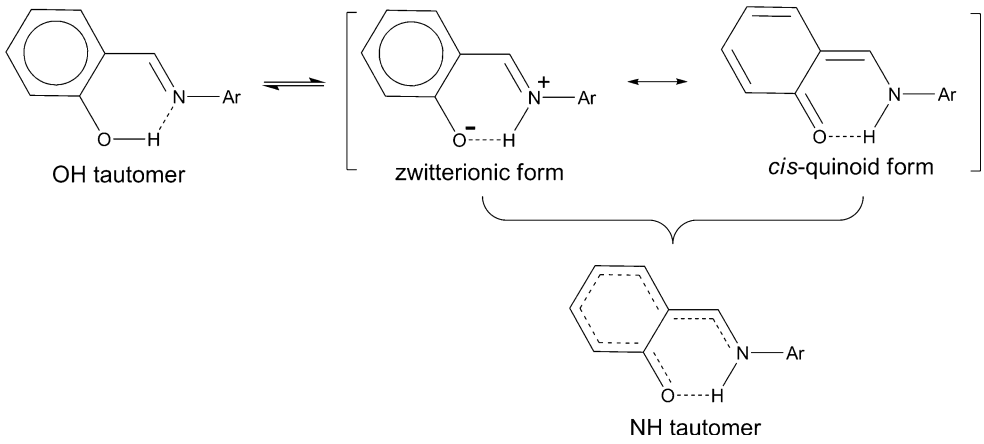

of their NH forms (Scheme 1), retaining the phenyl ring aromaticity and containing the protonated nitrogen atom. Thus, they have an ionic intramolecular hydrogen bond (N^+–H···O^-). Zwitterionic forms are easily distinguishable from the other NH forms, since N^+–H bonds are longer than the standard interatomic separations observed in neutral N–H bonds (0.87 Å) [9, 11–13]. The other ionic bonds in the zwitterions, C–O^- and C=N^+, are not as distinctive as N^+–H bond to define the tautomeric form, because NH tautomer can be regarded as a resonance hybrid of two canonical structures, the *cis*-quinoid and zwitterionic forms, as shown in Scheme 1 [14]. Although NH forms of *o*-hydroxy Schiff bases seem to be the same as each other in terms of atomic positions, their covalent skeletons are different, since π-electron delocalization situation is a driving force affecting tautomeric equilibria of *o*-hydroxy Schiff bases. Considering other tautomeric forms, it can be stated that OH and NH forms of *o*-hydroxy Schiff bases may coexist in the same crystal structure [15] or in the same molecular structure [16]. In general, *o*-hydroxy Schiff bases in NH form exist as resonance hybrid of zwitterionic and *cis*-quinoid [16] or OH and *cis*-quinoid tautomers [17, 18]. Electronic π-delocalization in the chelate ring facilitates to stabilize such molecules and determines the type of tautomer. Experimental verification of this model is difficult, because keto and phenol tautomer of the compound are not sufficiently distinguishable from each other due to positional disorder when the tautomeric protons are located at the midpoint of the hydrogen bridge between O and N. In this study, distinct molecular geometries at the different stages in tautomerism of the title compound have been crystallographically examined and physical reasons underlying intramolecular proton transfer process has been investigated by quantum chemical calculations. Since modeling studies for tautomerism in salicylideneaniline derivatives by nonadiabatic proton transfer using a redundant internal coordinate have been introduced recently [19], the present treatise is of importance for relevant scientific community.

Experimental

Synthesis of the title compound

The compound (*E*)-2-ethoxy-6-[(2-methoxyphenylimino)methyl]phenol (Scheme 2) was prepared by reflux a mixture of a solution containing 3-ethoxysalicylaldehyde (0.5 g 3 mmol) in 20-mL ethanol and a solution containing 2-methoxyaniline (0.369 g 3 mmol) in 20-mL ethanol. The reaction mixture was stirred for 1 h under reflux. The crystals of (*E*)-2-ethoxy-6-[(2-methoxyphenylimino)methyl]phenol suitable for X-ray analysis were obtained from tetrahydrofuran by slow evaporation (yield % 72; m.p. 356–358 K).

X-ray crystallography

A brown-colored prism-shaped crystal sample with dimensions of 0.72 × 0.48 × 0.2 mm^3 was chosen for the crystallographic study. The intensity data were collected on a STOE IPDS 2 diffractometer using graphite

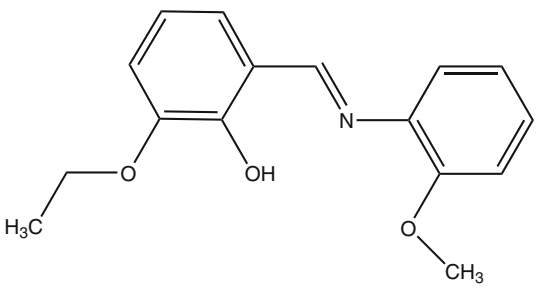

Scheme 2 Chemical chart of the title compound, $C_{16}H_{17}NO_3$

Table 1 Crystallographic data and parameters of refinement process for the title compound $C_{16}H_{17}NO_3$ at 296 and 100 K

	296 K	100 K
Formula weight	271.31	271.31
Cell setting, space group	Monoclinic, $P2_1/c$	Monoclinic, $P2_1/c$
Unit cell parameters	$a = 12.9000(6)$ Å	$a = 12.6417(4)$ Å
	$b = 28.3595(19)$ Å	$b = 28.6543(14)$ Å
	$c = 11.8826(5)$ Å	$c = 11.6173(4)$ Å
	$\beta = 94.031(4)°$	$\beta = 95.053(3)°$
Volume (Å^3)	4336.3(4)	4191.9(3)
Z	12	12
Absorption coefficient (μ)	0.086 mm^{-1}	0.089 mm^{-1}
T_{min}, T_{max}	0.952, 0.983	0.948, 0.982
θ range for data collection	1.44°–26.04°	1.42°–26.05°
h_{min}, h_{max}	−14, 15	−13, 15
k_{min}, k_{max}	−34, 34	−35, 35
l_{min}, l_{max}	−14, 14	−14, 14
Number of reflections collected	46653	48455
Independent/observed reflections	8509/3298	8226/5739
Data/restraints/parameters	8509/10/572	8226/0/560
Extinction Coefficient	0.0010(1)	0.0017(2)
Goodness of fit on F^2	0.770	0.942
Final R indices [$I > 2\sigma(I)$]	$R_1 = 0.038$	$R_1 = 0.036$
	$\omega R_1 = 0.074$	$\omega R_1 = 0.081$
$\Delta\rho_{max}$, $\Delta\rho_{min}$ (e Å^{-3})	0.095, −0.125	0.180, −0.165

monochromated MoK$_\alpha$ radiation ($\lambda = 0.71073$ Å) at 296 and 100 K in the ω scan mode and cell parameters were determined using X-AREA software [20]. The systematic absences and intensity symmetries indicated the monoclinic $P2_1/c$ space group at both the temperatures. Intensity data collected at both the temperatures were corrected for absorption effects by the integration method via X-RED software [20]. Other details of the data collection conditions and parameters of refinement process are summarized in Table 1. The structures at 296 and 100 K were solved by direct methods using SHELXS-97 [21]. The refinement was carried out by full-matrix least-squares method on the positional and anisotropic thermal parameters of the nonhydrogen atoms, equivalently corresponding to 572 crystallographic parameters at 296 K and to 560 crystallographic parameters at 100 K. The scattering factors were taken from SHELXL-97 [21]. For both the temperatures, all nonhydrogen atoms were refined anisotropically and all H atoms except for H1 atoms for the three molecules in the asymmetric unit were positioned geometrically and treated using suitable riding models, fixing the aromatic C–H distances at 0.93 Å, the methylene C–H distances at 0.97 Å [U_{iso}(H) = 1.2 U_{eq}(C)], and the methyl C–H distances at 0.96 Å [U_{iso}(H) = 1.5 U_{eq}(C)].

Treatment of the tautomeric hydrogens

The difference-Fourier synthesis located one peak to be attributed to tautomeric hydrogen atoms (H1) for each molecule in the asymmetric unit. Since these peaks were located at midpoints of hydrogen bridges between O1 and N1 at 296 K, it is hard to determine precisely the parent atoms of tautomeric hydrogen atoms. Due to ambiguity in positions of the H1 atoms at 296 K, these atoms were treated as positional disordered in the refinement process using SUMP restraints on their site occupancy factors (s.o.f.), so that different assignments to the partitions of site occupancy factors of the disordered H-atom pairs make possible. After the final refinement cycle, the s.o.f. values of H1a (O1a) and H1b (N1a) in molecule A are 0.62(3) and 0.38(3), respectively; H1c (O1b) and H1d (N1b) in molecule B are 0.58(3) and 0.42(3), respectively; H1e (O1c) and H1f (N1c) in molecule C are 0.48(3) and 0.52(3), respectively. The tautomeric H-atoms at 100 K were located in difference Fourier map and refined independently.

Supplementary data Crystallographic data excluding structure factors for the structures reported in this article have been deposited with the Cambridge Crystallographic Data Centre as supplementary publication numbers CCDC 711348 and 711349. Copies of the data can be obtained

free of charge on application to CCDC, 12 Union Road, Cambridge CB2 1EZ, UK (Fax: (+44) 1223 336-033; e-mail: data_request@ccdc.cam.ac.uk).

Computational details

The geometry optimizations leading to in vacuo energy minima for OH and NH tautomers of the title molecule were performed using DFT calculations with B3LYP hybrid exchange correlation functional [22] by means of 6-31 + G(d,p) basis set implemented in Gaussian 03W program package [23]. The crystallographic coordinates were used as starting point in geometry optimizations. To be able to describe the potential barrier height for the intramolecular phenolic proton transfer, a relaxed Potential Energy Surface (PES) scan was performed based on the optimized geometry of OH tautomeric form at the B3LYP/6-31 + G(d,p) level by varying the redundant internal coordinate [O1–H1 bond] from 1.00 to 1.80 Å with 17 steps of 0.05 Å. All the remaining parameters were optimized at each step in the overall scan process, i.e., non-adiabatic approximation representing proton movement in hydrogen bridge. The HOMA indices [24] were calculated throughout the scan process to quantitatively express changes in the aromaticities of the rings involving proton transfer. HOMA index which is developed to quantitatively express aromaticity levels of a molecular moiety can be seen as a measure for π-electron delocalization level. Electronic absorption spectra for OH tautomeric form of the compound were calculated by time-dependent DFT (TD-DFT) method in ethanol, including solvent–solute interaction energy in the Hamiltonian of the system according to Polarizable Continuum Model (PCM) at the same level of theory [25].

Results and discussion

FT-IR spectrum of the compound

The IR spectrum was recorded by a Bruker Vertex 80V FT-IR spectrometer using KBr pellets in the 4000–400 cm^{-1} region. In the FT-IR spectrum of the compound, broad absorption band is observed in the 3050–2950 cm^{-1} region. This can be interpreted as a sign of the formation of an intramolecular hydrogen bond. Absorption bands between 1600 and 1700 cm^{-1} are due to stretching vibrations of C=N and C=O. In this region, both the bands were observed for the compound. Sharp and strong first band was observed at 1612.16 cm^{-1} ($\nu_{C=O}$) and the second band as a shoulder with weak intensity was located near the first band. This fact can be explained by the presence of $C=N^{+}H$ stretching motion from a zwitterionic structure (Scheme 1) [26, 27]. On the other hand, strong band at 1251.10 cm^{-1} can be ascribed to C_{ar}–OH stretching mode indicating high percentage of phenol-imine tautomeric form in solid state. In addition, moderate absorption band at 1173.60 cm^{-1} can be assigned to C–N stretching. Spectral results suggest that keto-amine and phenol-imine tautomer coexist and furthermore, zwitterionic form of the title compound is found in appreciable amounts as compared to the others. In this regard, it is required careful X-ray crystallographic study to properly determine tautomeric form of the title compound and their percentage in solid state.

Molecular structure at 296 K

There are three crystallographically independent molecules (referred to as molecule A, B, and C hereafter) in the asymmetric unit. An *ORTEP-3* [28] view is shown in Fig. 1. Selected bond distances at both the temperatures are given in Table 2. When the bond distances of the

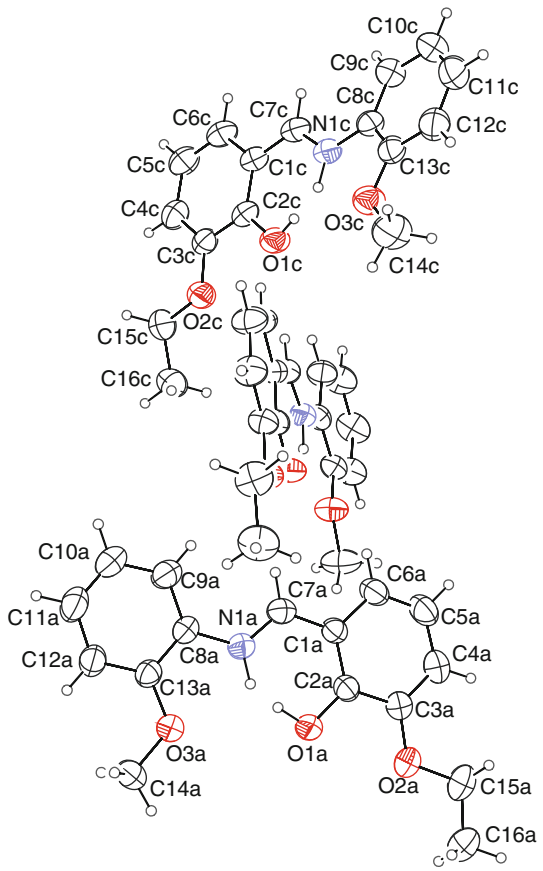

Fig. 1 An *ORTEP-3* view of the molecules in the asymmetric unit at 296 K. Displacement ellipsoids are drawn at the 30% probability level and H atoms are shown as small spheres of arbitrary radii. The tautomeric H atoms are disordered over O1 and N1 sites of each molecule in the asymmetric unit. An identical numbering scheme was applied to molecule B, but atoms in molecule B are not labeled for the sake of clarity

Table 2 Selected bond distances (Å) for the three molecules in the asymmetric unit at both temperatures

	A		B		C	
	100 K	296 K	100 K	296 K	100 K	296 K
C2–O1	1.353(2)	1.335(2)	1.342(2)	1.327(2)	1.343(2)	1.317(2)
C7–N1	1.295(2)	1.294(2)	1.295(2)	1.287(2)	1.289(2)	1.297(3)
C1–C7	1.444(2)	1.427(3)	1.444(2)	1.425(3)	1.440(2)	1.413(3)
C1–C2	1.403(2)	1.400(2)	1.408(2)	1.407(2)	1.409(2)	1.409(3)
C2–C3	1.408(2)	1.407(3)	1.411(2)	1.408(3)	1.408(2)	1.417(3)
C3–C4	1.381(2)	1.372(3)	1.379(2)	1.366(3)	1.377(2)	1.362(3)
C4–C5	1.396(2)	1.390(3)	1.401(2)	1.390(3)	1.399(2)	1.398(3)
C5–C6	1.370(2)	1.359(3)	1.370(2)	1.360(3)	1.370(2)	1.344(3)
C1–C6	1.4089(18)	1.404(3)	1.412(2)	1.406(3)	1.406(2)	1.414(3)
C8–N1	1.409(2)	1.413(2)	1.409(2)	1.415(2)	1.416(2)	1.418(3)
C3–O2	1.367(2)	1.363(2)	1.372(2)	1.371(2)	1.369(2)	1.367(2)
C13–O3	1.375(2)	1.367(2)	1.366(2)	1.366(2)	1.368(2)	1.356(2)
O2–C15	1.432(2)	1.407(2)	1.430(2)	1.427(2)	1.439(2)	1.417(2)
C15–C16	1.497(2)	1.479(3)	1.506(2)	1.498(3)	1.508(2)	1.499(3)
O3–C14	1.429(2)	1.426(2)	1.432(2)	1.431(2)	1.427(2)	1.431(3)

molecules A, B, and C in Table 2 are compared to those of other similar structures in the literature, it is seen that the molecules at 296 K are not of typical geometrical parameters of their two limiting tautomeric forms (phenol-imine or keto-amine) exactly, probably due to the intramolecular proton transfer process. While two of symmetry-independent molecules in the asymmetric unit, molecules A and B, are almost planar, molecule C slightly deviates from planarity. The dihedral angle between the C1/C6 and C8/C13 rings are 4.56(4)°, 6.69(14)°, and 14.54(13)° for molecule A, B, and C, respectively.

The heteroatom bonds are those most affected geometrical parameters by intramolecular proton transfer in *o*-hydroxy Schiff bases. Therefore, the C2–O1 and C7–N1 bonds are the most sensitive indicators of the tautomeric form for the compound. The C2–O1 bond is a single bond for the phenol-imine tautomer, whereas this bond displays double-bond character in keto-amine tautomer. The C7–N1 bond is also a double-bond in phenol-imine tautomer, whereas it is a single bond in canonical keto-amine tautomers (Scheme 1). The C2a–O1a [1.335(2) Å], C2b–O1b [1.327(2) Å] bonds are somewhat shorter; and C7a–N1a [1.294(2) Å], C7b–N1b [1.287(2) Å], and C7c-N1c [1.297(3) Å] bond distances are somewhat longer than those of compounds previously reported as phenol-imine (corresponding values for C2–O1; 1.350(2) Å [29], 1.359(3)–1.360(3) Å [30], 1.346(4) Å [31], and for C7–N1; 1.277(2) Å [29], 1.286(3) Å [30], 1.270(5) Å [31]). The C2c–O1c [1.317(2) Å] bond distance is quite shorter than those of phenol-imine tautomer and longer than those for similar keto-amine tautomer (1.293(2) Å [32], 1.286(5) Å [33], 1.291(2) Å [34]). It can be said that this bond distance is intermediate between single and double C to O. Furthermore, the C1a–C7a [1.427(3) Å], C1b–C7b [1.425(3) Å], and C1c–C7c [1.413(3) Å] bond distances are somewhat shorter than those of compounds reported as phenol-imine in the literature (1.443(2) Å [29], 1.454(5) Å [31]). This bond is also a double bond for keto-amine taoutomer (1.391(6) Å [33], 1.404(2) Å [32]). For each molecule in the asymmetric unit, the ambiguity in positions of the tautomeric H1 atoms in the difference-Fourier maps at 296 K supports this conclusion. These atoms were treated as disordered in the refinement process. After the final refinement cycle, the s.o.f. values of the tautomeric hydrogen atoms attached to O1 atoms are 0.62(3), 0.58(3), and 0.48(3) for molecules A, B, and C, respectively. According to these values, it can be said that the molecules A and B predominantly exist in OH (phenol-imine) form with the respective 62 and 58% probability level. The disordered H1 atoms attached to O1c and N1c atoms have close s.o.f. values of 48 and 52%, respectively.

Aromaticities of molecular fragments possessing π-delocalized systems are defined quantitatively by structural Harmonic Oscillator Model of Aromaticity (HOMA) index [24]. HOMA index is defined by the following equation:

$$\mathrm{HOMA} = 1 - \left[\frac{1}{n}\sum_{j=1}^{n} \alpha_j \left(R_j - R_{\mathrm{opt}}\right)^2\right],$$

where n is the number of bonds taken into the summation, R_js stand for individual bond lengths, α_j regarded as a normalization constant is equal to 257.7 for C–C, 93.52 for C–N, and 157.38 for C–O bonds, fixed to give HOMA = 0 for nonaromatic Kekulé systems and HOMA = 1 for purely aromatic systems with all bonds equal to the optimal

value R_{opt} = 1.388 Å for C–C, R_{opt} = 1.334 Å for C–N, and R_{opt} = 1.265 Å for C–O [24].

It is well known that the C1/C6 ring is aromatic for phenol-imine tautomer and zwitterionic form. In order to investigate quantitatively the differences between the aromaticities of the three phenol (C1/C6) rings during intramolecular proton transfer, their harmonic oscillator model of aromaticity (HOMA) indices [24] were calculated. The calculated HOMA index of phenol ring is 0.92 for molecule A, 0.90 for molecule B, and 0.80 for molecule C. Comparing these values with the HOMA index calculated for canonic benzene (1.001) [35], it can be stated that π-electron delocalizations of aromatic rings involving proton transfer are considerably deformed, however, the deviation from full aromaticity of phenol ring in molecule C is more pronounced than those of molecules A and B. Keeping in mind that each of the molecules in the asymmetric unit can be regarded as a superposition of two limiting tautomeric form and considering the deformations in aromaticities of the phenol rings, it can be stated that OH tautomeric character of molecules A and B is more pronounced than that of molecule C.

Molecular structure at 100 K

In order to determine the positions of tautomeric H1 atoms properly and to avoid the uncertainties in the positions of tautomeric H atoms, the crystal structure of the title compound was also determined at 100 K whose molecular orientations are very similar those in Fig. 1. According to the positions of tautomeric H atoms and indicative bond distances, it can be clearly seen that three molecules in the asymmetric unit adopt phenol-imine (OH) tautomeric form at 100 K. Selected bond distances are listed in Table 2. The dihedral angle between the C1/C6 and C8/C13 rings are 9.29(3)°, 5.69(9)°, and 25.53(8)° for molecules A, B, and C, respectively. Considering deviation from planarity of the molecules in the asymmetric unit, it is seen that planarity of molecules A and C is increased, while that of molecule B is decreased with increasing temperature.

It can be seen that most of the bond distances at 100 K are slightly longer than those found at 296 K (Table 2), but this is to be expected due to the thermal motion model. There are also O–H···N type strong intramolecular hydrogen bonds in each molecule in the asymmetric unit (Table 3) and the O1···N1 distances are significantly shorter than the sum of the van der Waals radii for N and O atoms (3.07 Å) [36]. Besides intramolecular hydrogen bonds, there are three weak C–H···π interactions in the crystal structure at 100 K (for more information about the crystal structure at both temperatures, please see Electronic supplemental material).

Table 3 Intramolecular hydrogen bonding geometries (Å, °) for the title compound at 100 K

D–H···A	D–H	H···A	D···A	∠D–H···A
O1a–H1a···N1a	1.02(2)	1.58(2)	2.535(2)	154.1(2)
O1b–H1b···N1b	1.02(2)	1.56(2)	2.511(1)	153(2)
O1c–H1c···N1c	1.00(2)	1.61(2)	2.546(2)	153(2)

Computational study

The DFT calculations show that the NH form of the title molecule is less stable than its OH form in the gas phase. The energy difference between them is ca. 2.59 kcal/mol. Selected bond distances, bond angles, and torsion angles of the DFT optimized OH molecule are given in Table 4.

In order to better understand the proton transfer phenomenon in this molecule, the potential barrier for the transfer of the phenolic proton was calculated. DFT calculation in the gas phase predicts the potential barrier as

Table 4 Selected bond distances (Å), bond angles (°) and torsion angles (°) calculated with DFT at the B3LYP/6-31 + G(d,p) level of OH form of the title compound $C_{16}H_{17}NO_3$

C2–O1	1.339
C7–N1	1.292
C1–C7	1.451
C1–C2	1.417
C2–C3	1.421
C3–C4	1.393
C4–C5	1.408
C5–C6	1.382
N1–C7–C1	122.171
C7–N1–C8	121.745
O1–C2–C1	122.495
C1–C7–N1–C8	176.799
C6–C1–C7–N1	−178.786
C13–C8–N1–C7	147.036
C1–C6	1.415
C8–N1	1.403
C3–O2	1.362
C13–O3	1.362
O2–C15	1.428
C15–C16	1.519
O3–C14	1.422
C2–C1–C7	120.614
C13–C8–N1	117.796
O3–C13–C8	115.763
C7–C1–C2–O1	0.306
C8–C13–O3–C14	177.778
C16–C15–O2–C3	179.700

4.98 kcal/mol (Fig. 2). This barrier is probably altered in the crystal structure due to the geometrical discrepancies and intermolecular interactions. Nonetheless, this barrier height is sufficiently small so that proton transfer is easily occurred as compared to those of *o*-hydroxy aryl Schiff bases, which are less than 5 kcal/mol [37]. In this sense, formation of intramolecular H-bond of the title compound can be classified as low-barrier H-bond (LBHB).

Variations of the indicative bond distances throughout the PES scan process are shown in Fig. 3. It can be seen that these bonds change so as to adopt ultimately the keto-amine form of the title molecule. However, indicative bond lengths C2=O1 [1.259 Å] and C1=C7 [1.396 Å] belonging to stable NH tautomer at the sixteenth scan step are different from their expected values of 1.222 and 1.333 Å in benzoquinones, respectively [38], whereas C7–N1 bond length [1.335 Å] at the sixteenth scan step is close to its corresponding value of 1.339 Å [38]. While C2–O1 and C7=N1 bonds become double- and single-bond during the tautomerization, respectively, single-bond character of C2–C3 is more pronounced than that of C1–C6 and C1–C2.

Variation of the HOMA indices belonging to phenol and chelate ring depending on the scan coordinate are shown in Fig. 4a. It is seen that the aromaticty of chelate ring is increasing up to distance value of 1.25 Å contrary to that of phenol ring. After this critical point, aromaticities of both fragments are starting to decrease, however, that of phenol ring is decreasing remarkably. In addition to this, considering the variation of HOMA indices belonging to anisole ring shown in Fig. 4b, it is obvious that the aromaticity of anisole ring is increasing at least in a narrow interval. These different behaviors of each fragment can only be

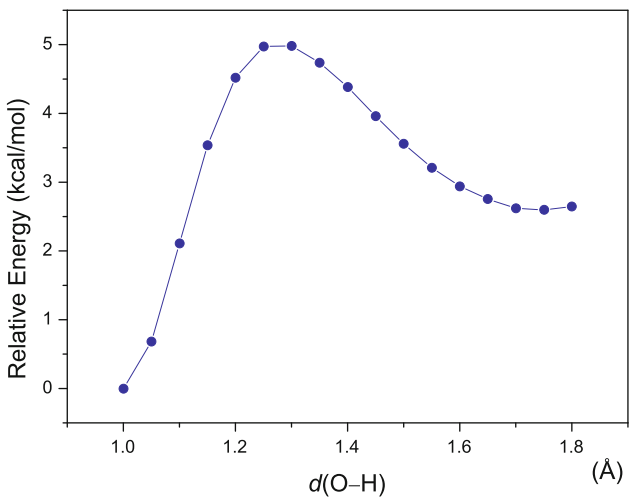

Fig. 2 Relative energies of the tautomers with respect to the energy minimized conformer of the title compound versus the redundant coordinate O1–H1 bond distance in PES scan process. Here relative energy values are calculated with respect to the absolute minimum for which $E = -900.402$ au

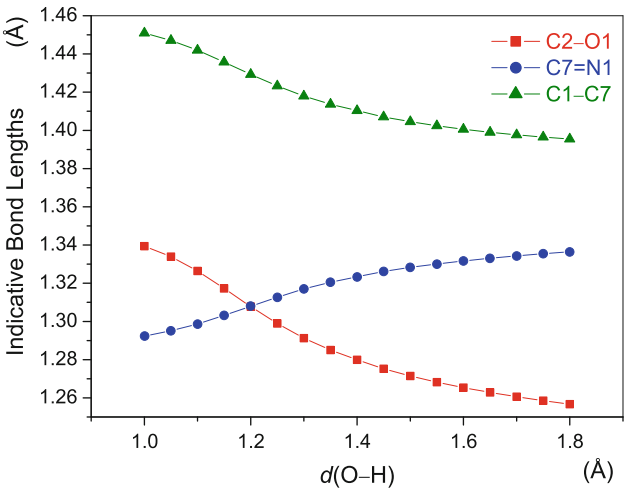

Fig. 3 Variations of the indicative bond lengths versus the scan coordinate *d*(O–H)

explained by the fact that the loss in aromaticity of the phenol ring is compensated by augmentation in aromaticity of the chelate ring under the value of 1.25 Å of the scan coordinate. Furthermore, synchronous decreasing in aromaticities of these adjacent fragments beyond this value causes an increase in aromaticity of the anisole ring. Similar tendencies are observed for another *o*-hydroxy aromatic Schiff base, (*Z*)-6-((4-bromophenylamino) methylene)-2,3-di-hydroxycyclohexa-2,4-dienone [19]. It can be mentioned here the presence of long-ranged π-electron coupling for the title compound so that π-electrons transfer from phenol toward anisole ring by means of chelate ring.

The mentioned charge transfer through π-orbitals followed by aromaticity levels of the adjacent phenol and chelate ring are generally verified by considering the relevant aromaticity levels obtained from X-ray crystallographic study given in Table 5. HOMA values of phenol rings in *o*-hydroxy aryl and naphthaldimine Schiff bases in OH tautomeric form are in the interval of 0.90–0.99 [37, 39–41]. In Schiff base species in NH tautomeric form, while HOMA values of the six-membered rings carrying O atom in *ortho* position vary from 0.50 to 0.80 [39]. On the other hand, while pseudo-aromaticity of the chelate ring changes within the interval of 0.20–0.50 approximately for Schiff base species derived from naphthaldimine [39], it varies from 0.208 to 0.462 for OH and from 0.651 to 0.942 for NH forms of *o*-hydroxy aryl Schiff bases [37]. HOMA values of phenol ring in the optimized OH and NH tautomer of the title compound are found as 0.867 and 0.259. In addition, pseudo-aromaticity of the chelate ring in the optimized OH tautomer of the title compound (0.432) is less than that of the energy minimized NH tautomer (0.609) as shown in Fig. 4a. These results are in agreement with those by Filarowski et al. As can be seen from the results in Table 5, intramolecular charge transfer is also

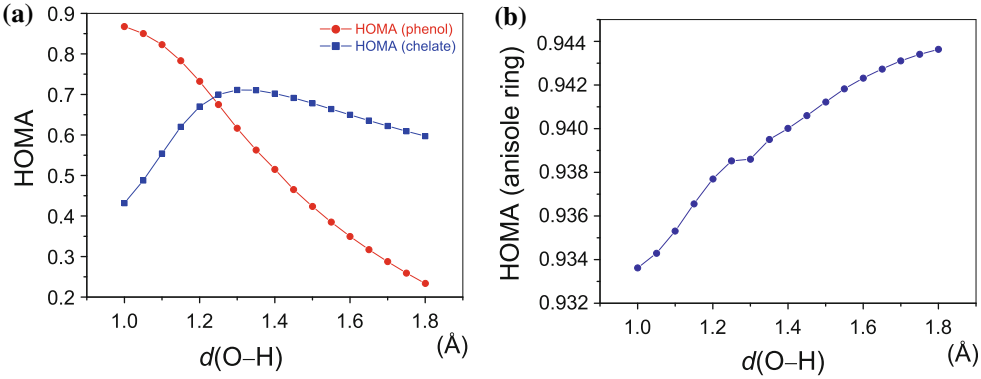

Fig. 4 Dependence of HOMA values of the adjacent rings involving proton transfer (**a**) and anisole ring (**b**) against the scan coordinate *d*(O–H)

Table 5 HOMA indices for certain fragments with respect to the crystallographically observed geometries of the title molecule

	HOMA (phenol)			HOMA (chelate)			HOMA (anisole)		
	A	B	C	A	B	C	A	B	C
100 K	0.936	0.912	0.925	0.444	0.505	0.509	0.977	0.980	0.981
296 K	0.920	0.899	0.799	0.663	0.686	0.793	0.951	0.944	0.909

affected by temperature. While π-electron donation from phenol to chelate ring is increased with increasing temperature, electronic charge transfer from chelate to anisole ring is somewhat decreased with increasing temperature.

Electronic absorption spectra were recorded in EtOH between 200 and 600 nm on a Unicam V2-100 UV–VIS spectrophotometer, using 1-cm quartz cells at the room temperature. There are two evident absorption bands at 270 nm ($\log \varepsilon = 2.65$) and at 340 nm ($\log \varepsilon = 2.72$). Another band observed at 461 nm ($\log \varepsilon = 1.93$) can be assigned to n–π^* transition indicating partial keto-amine character of the title compound [14]. FMO analysis can be used to estimate the origins of the peaks in UV–Vis spectrum. Calculated π–π* absorption bands in ethanol are observed at and 272 and 337 nm. Energy gap between HOMO and LUMO is 3.816 eV for stable OH tautomer. Highest occupied molecular orbital (HOMO) and lowest unoccupied molecular orbital (LUMO) are shown in Fig. 5. HOMO is predominantly localized on phenol rings, whereas LUMO is almost localized overall molecule. While the first band at 272 nm is primarily due to electronic charge transition from HOMO-3 to LUMO, the second at 337 nm is originated from transition between HOMO-1 and LUMO. It is inferred from FMO analysis that both the absorption bands below 400 nm may be attributed to π–π* transitions between aromatic rings through the imine functionality. Comparing these values with the corresponding experimental values, it can be stated that TD-DFT within PCM framework is a useful tool for estimation UV–Vis spectrum.

Intramolecular hydrogen bonding is of great importance in understanding details of charge transfer properties in the title compound, since pseudo-aromatic chelate ring formation is established by decreasing in phenol ring aromaticity. Estimating H-bond dissociation energy E_{HB} is usually a laborious task because of the fact that many different conformers as a result of H-bonding are possible. A useful exponential model in order to describe H-bond dissociation energy in terms of geometrical parameters in the H-bond region has been put forward by Musin and Mariam [42]. According to Musin and Mariam approach, intramolecular H-bond dissociation energy E_{HB} estimated by the following empirical relationship;

$$E_{HB} = 5.554 \times 10^5 \exp(-4.12 d_{D\cdots A}),$$

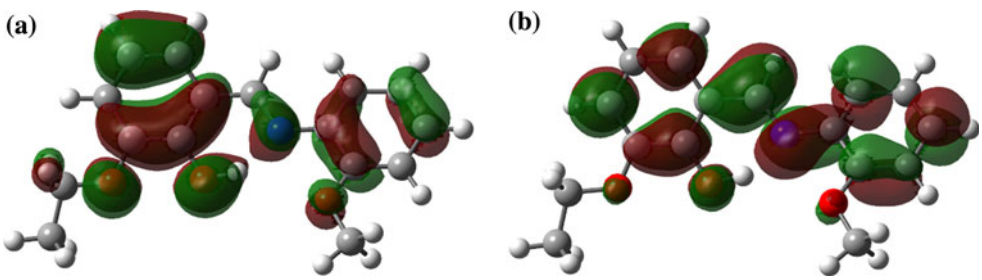

Fig. 5 HOMO (**a**) and LUMO (**b**) for phenol-imine tautomer of the title compound in gas phase

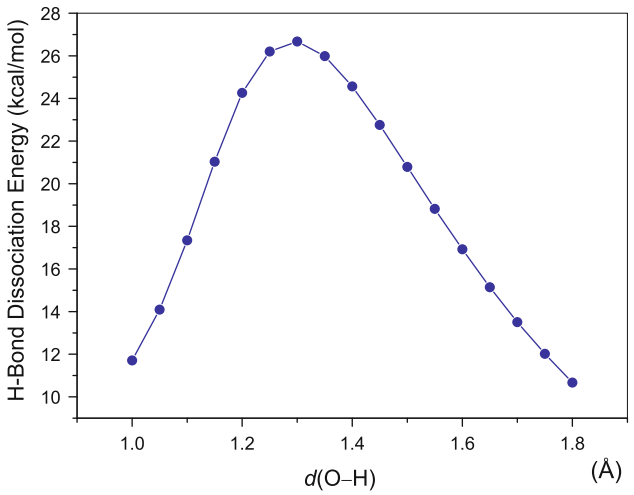

Fig. 6 Variation of intramolecular H-bond dissociation energy of the title compound

where $d_{D\cdots A}$ denotes the distance between the donor (D) and acceptor (A) atom involving intramolecular H-bond. Dependency of intramolecular H-bond dissociation energy of the title compound is shown in Fig. 6. According to Fig. 6, the most strength H-bonds are observed for transition states (TSs) which tautomeric proton is almost located at the midpoint of the hydrogen bridge. This result is in agreement with Leffler–Hammond rule [43, 44], declaring that the systems closer to TSs the stronger H-bonds than those species far from TSs. This result is experimentally confirmed by Filarowski et al. for distinct *o*-hydroxyaryl Schiff base species in Refs. [37, 39–41]. H-bond dissociation energies of stable OH and NH form (at the sixteenth step) of the title compound are approximately found as 12 kcal/mol and these values are comparable the corresponding values obtained for *o*-hydroxy aryl Schiff bases reported in [45]. Considering only the distances between the donor and acceptor atom, it can be stated that intramolecular H-bonds in the title compound at both the temperatures can be regarded as low-barrier hydrogen bonds (LBHB), since the corresponding distances of O–H···N (or O···H–N)- type LBHBs are less than 2.65 Å [37]. Distances between the donor and acceptor atoms are below 2.65 Å at both 100 and 296 K. This is in agreement with the fact that the potential barrier height (4.98 kcal/mol) is sufficiently small and therefore tautomeric proton can be easily transferred to N atom in imine bridge.

Conclusions

The results from FT-IR and UV–Vis suggest that both tautomeric forms of the compound coexist in solid state and solution. Tautomeric equilibrium in solid state is examined by X-ray crystallographic study. Changes in both covalent skeleton of the title compound accompanying proton transfer were monitored by nonadiabatic PES scan with respect to hydroxyl bond length. Quantum chemical studies for the compound suggest that pseudo-aromatic chelate ring formation causes to a decrease aromaticity (or π-electron delocalization) in phenol ring, reflecting a dynamic equilibrium between aromaticities of these adjacent fragments. In addition, further aromatization of anisole ring during proton transfer reaction suggests the presence of π-electron coupling affecting overall molecule. Since the calculated potential energy barrier is sufficiently small to transfer tautomeric proton from O to N as compared to previously reported values for *o*-hydroxy aryl Schiff bases, intramolecular H-bond in the compound may be seen as a LBHB. These conclusions are experimentally verified by X-ray crystallographic studies at 296 and 100 K. Charge transfer from phenol ring to pseudo-aromatic chelate ring increases with increasing temperature, whereas π-electron transfer from chelate ring to anisole ring is decreased as temperature increases.

Acknowledgment The authors wish to acknowledge Ondokuz Mayıs University for the use of the STOE IPDS 2 diffractometer purchased under grants F.279 and F.377.

References

1. Canali L, Sherrington DC (1999) Chem Soc Rev 28:85–93
2. Gibson VC, Spitzmesser SK (2003) Chem Rev 103:283–315
3. Rousso I, Friedman N, Sheves M, Ottolenghi M (1995) Biochemistry 34:12059–12065
4. Lanyi JK (1993) Biochim Biophys Acta 1183:241–261
5. Das K, Sarkar N, Ghosh AK, Majumdar D, Nath DN, Bhattacharyya K (1994) J Phys Chem 98:9126–9132
6. Fores M, Duran M, Sola M, Orozco M, Luque FJ (1999) J Phys Chem A 103:4525–4532
7. Acuna AU, Amat Guerri F, Costela A, Douhal A, Figuera JM, Florido F, Sastre R (1991) Chem Phys Lett 187:98–102
8. Nishiya T, Yamauchi S, Hirota N, Baba M, Hanazaki I (1986) J Phys Chem 90:5730–5735
9. Wojciechowski G, Ratajczak-Sitarz M, Katrusiak A, Schilf W, Przybylski P, Brzezinski B (2003) J Mol Struct 650:191–199
10. Mondal B, Lahiri GK, Naumov P, Ng SW (2002) J Mol Struct 613:131–135
11. Petek H, Albayrak C, Agar E, Kalkan H (2006) Acta Crystallogr E62:o3685–o3687
12. Petek H, Albayrak C, Ocak-Iskeleli N, Agar E, Senel I (2007) J Chem Crystallogr 37:285–290
13. Steiner T (1998) J Phys Chem A 102:7041–7052
14. Ogawa K, Harada J (2003) J Mol Struct 647:211–216
15. Nazır H, Yıldız M, Yılmaz H, Tahir MN, Ülkü D (2000) J Mol Struct 524:241–250
16. Karabiyik H, Guzel B, Aygun M, Boga G, Buyukgungor O (2007) Acta Crystallogr C63:o215–o218
17. Ligtenbarg AGJ, Hage R, Meetsma A, Feringa BL (1999) J Chem Soc Perkin Trans 2:807–812

18. Karabiyik H, Ocak-Iskeleli N, Petek H, Albayrak C, Agar E (2008) J Mol Struct 873:130–136
19. Karabiyik H, Petek H, Iskeleli NO, Albayrak C (2009) Struct Chem 20:1055–1065
20. Stoe & Cie (2002) X-AREA (Version 1.18) and X-RED32 (Version 1.04), Darmstadt, Germany
21. Sheldrick GM (2008) Acta Crystallogr A64:112–122
22. Hertwig RH, Koch W (1997) Chem Phys Lett 268:345–351
23. Frisch MJ, Trucks GW, Schlegel HB, Scuseria GE, Robb MA, Cheeseman JR, Montgomery JA, Vreven T Jr, Kudin KN, Burant JC, Millam JM, Iyengar SS, Tomasi J, Barone V, Mennucci B, Cossi M, Scalmani G, Rega N, Petersson GA, Nakatsuji H, Hada M, Ehara M, Toyota K, Fukuda R, Hasegawa J, Ishida M, Nakajima T, Honda Y, Kitao O, Nakai H, Klene M, Li X, Knox JE, Hratchian HP, Cross JB, Bakken V, Adamo C, Jaramillo J, Gomperts R, Stratmann RE, Yazyev O, Austin AJ, Cammi R, Pomelli C, Ochterski JW, Ayala PY, Morokuma K, Voth GA, Salvador P, Dannenberg JJ, Zakrzewski VG, Dapprich S, Daniels AD, Strain MC, Farkas O, Malick DK, Rabuck AD, Raghavachari K, Foresman JB, Ortiz JV, Cui Q, Baboul AG, Clifford S, Cioslowski J, Stefanov BB, Liu G, Liashenko A, Piskorz P, Komaromi I, Martin RL, Fox DJ, Keith T, Al-Laham MA, Peng CY, Nanayakkara A, Challacombe M, Gill PMW, Johnson B, Chen W, Wong MW, Gonzalez C, Pople JA (2004) Gaussian 03, Revision E.01. Gaussian Inc., Wallingford
24. Krygowski TM (1993) J Chem Inf Comput Sci 33:70–78
25. Cossi M, Barone V, Robb MA (1999) J Chem Phys 111:5295–5302
26. Salman SR, Saleh NAI (1997) Spectr Lett 30:1289–1300
27. Aton B, Doukas AG, Narva D, Callender RH, Dinur U, Honig B (1980) Biophys J 29:79–94
28. Farrugia LJ (1997) J Appl Cryst 30:565
29. Yuce S, Ozek A, Albayrak C, Odabasoglu M, Buyukgungor O (2004) Acta Crystallogr E60:o718–o719
30. Temel E, Albayrak C, Odabasoglu M, Buyukgungor O (2007) Acta Crystallogr E63:o374–o376
31. Şahin O, Büyükgüngör O, Albayrak Ç, Odabaşoğlu M (2005) Acta Crystallogr E61:o1288–o1290
32. Şahin O, Büyükgüngör O, Albayrak Ç, Odabaşoğlu M (2005) Acta Crystallogr E61:o1579–o1581
33. Şahin O, Albayrak Ç, Odabaşoğlu M, Büyükgüngör O (2005) Acta Crystallogr E61:o2859–o2861
34. Petek H, Albayrak C, Odabasoglu M, Senel I, Buyukgungor O (2008) J Chem Crystallogr 38:901–905
35. Matito E, Duran M, Solà M (2005) J Chem Phys 122:014109-1/8
36. Bondi A (1964) J Phys Chem 68:441–451
37. Filarowski A, Koll A, Glowiak T (2002) J Chem Soc Perkin Trans 2:835–842
38. Allen FH, Watson DG, Brammer L, Orpen AG, Taylor R (2004) In: Prince E (ed) International tables for crystallography (vol. C): mathematical, physical and chemical tables, 3rd edn. Kluwer, Dordrecht, pp 790–811
39. Filarowski A, Kochel A, Kluba M, Kamounah FS (2008) J Phys Org Chem 21:939–944
40. Filarowski A (2005) J Phys Org Chem 18:686–698
41. Filarowski A, Kochel A, Cieslik K, Koll A (2005) J Phys Org Chem 18:986–993
42. Musin RN, Mariam YH (2006) J Phys Org Chem 19:425–444
43. Leffler JE (1953) Science 117:340–341
44. Hammond GS (1955) J Am Chem Soc 77:334–338
45. Filarowski A, Majerz I (2008) J Phys Chem A 112:3119–3126